

Application of the independent molecule model to the calculation of free energy and rigid-body motions of water hexamers

Shuzo Yoshioki

Yatsushiro National College of Technology, Yatsushiro 866-8501, Japan

Received 2 August 2002; accepted 14 November 2002

Abstract

The stabilities of five water hexamers (cyclic, boat, book, prism and cage structure) in the gas phase were investigated with the independent molecule model. In this model, the position and orientation of each water molecule within the hexamer are characterized with a translational vector and Eulerian angles, and then each molecule can move freely as a rigid body with respect to the others. Force field energy minimization yielded structures for each hexamer. Normal mode analyses were done on the five hexamers. Hydrogen bond strength in the hexamer decreases in the order: boat, cyclic, book, cage and prism. Hydrogen bond lifetimes also decrease in this order. By estimating the internal energy and the vibrational entropy of rigid-body motions, we determined the temperature dependence of the free energy for each hexamer in the range 100–350 K. Free energy of the hexamers increases in the previously mentioned order also. The most stable hexamer is the boat, and the least stable is the prism. The stabilities of the boat and the cyclic are very similar. The more planar hexamers (cyclic and boat) are more stable than the three-dimensional hexamers (cage and prism). Although the experiments of Liu et al. [Nature 381 (1996) 501] were interpreted in terms of a cage cluster, our calculations indicate boat is more likely.

© 2002 Elsevier Science Inc. All rights reserved.

Keywords: Water hexamer; Hydrogen bond strength and lifetime; Vibrational entropy; Free energy of water cluster; Thermal ellipsoid; Frequency of rigid-body motion

1. Introduction

In a previous study [1], we reported a new model to investigate internal and rigid-body motions of a protein in solution. This independent molecule model (independent MM) treats each molecule in the protein–water system as an independent molecule. Here we apply this model to water clusters. In the last 10 years, small water clusters have been studied extensively both experimentally and theoretically [2–17]. There is now general agreement that the global minima of the trimer, tetramer and pentamer are simple cyclic structures and that the octamer and larger clusters prefer three-dimensional (polycyclic) structures.

The five structures of the water hexamer have been investigated from mainly a theoretical point of view. Liu et al. [14] named these five configurations: cyclic, boat, book, prism and cage. It is useful to briefly review the main results of three separate theoretical studies.

1. Clementi and co-workers [10] did calculations of the binding energies for cyclic and prism structures using density functional theory. Optimizing both structures,

they found the binding energy of the prism structure is lower by 1.4 kcal/mol than for the cyclic structure (−39.88 kcal/mol), but they found after including zero-point energy corrections that the cyclic structure has the lower energy than the prism.

2. Masella and Flament [17] estimated the binding energies of the five hexamers using three theoretical models to study the interaction among water molecules. With a classical many-body polarization model, the cyclic structure has the lowest binding energy (−44.33 kcal/mol). With a topological and classical many-body polarization effects model, the book structure has the lowest energy (−48.89 kcal/mol). With a pairwise model, the prism structure has the lowest energy (−38.55 kcal/mol). Thus, the three models produced different energy results.
3. Liu et al. [14] tried to calculate the binding energies for five structures with a diffusion quantum Monte Carlo method. Using energy minimizations, they showed that the prism structure has the lowest energy, but the cage structure becomes slightly more stable when quantum vibrational zero-point energy corrections are properly taken into account. The authors also performed experiments of terahertz laser vibration-rotation tunneling spectroscopy of the structure of the water hexamer. Both cage and boat

E-mail address: yoshioki@as.yatsushiro-nct.ac.jp (S. Yoshioki).

structures are candidates to explain the experimental values, and the authors concluded that the water hexamer is more likely a cage rather than a boat based on energetic considerations. The three research groups thus did not reach a consensus.

We address the following points. Within the hexamer, each water molecule, treated as a rigid body, is fluctuating subject to hydrogen-bonding (H-bonding) and is undergoing internal motions. The entropies from the rigid-body motions must be included in the energy calculation. What we really want is the free energy including the entropy term, not just the binding energy.

In this article, we report the calculation of the free energy of the hexamers with the independent MM from our earlier article. We also evaluate the temperature dependence of the free energy. In addition, we discuss a relationship between the H-bond strength and the H-bond lifetime within each hexamer.

2. Methods

2.1. Independent molecule model

2.1.1. Independent variables

The independent variables in an independent MM are depicted in Fig. 1. The S-system is a fixed laboratory coordinate system. Each water molecule moves freely as a rigid body: six variables specify position and orientation of each molecule. The position and orientation of the k th water molecule with respect to the S-system is specified by

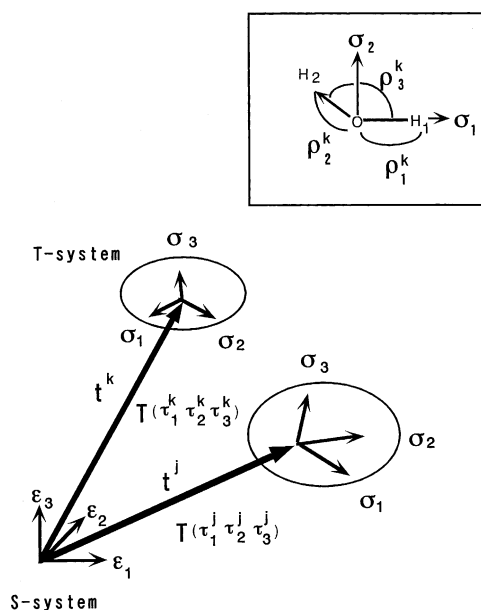


Fig. 1. The S-system is a fixed laboratory coordinate system. The T-system is on a water molecule. The two water molecules are modelled. Inset: the oxygen atom in a water molecule is placed at the origin of the T-system, and H₁ atom is on the positive x -axis, and H₂ atom lies on the plane spanned by σ_1 and σ_2 .

Table 1

Nonbonded potential parameters $U_{NB} = \epsilon(r_0/r_{ij})^{12} - 2.0\epsilon(r_0/r_{ij})^6$		
Atom pairs (i, j)	ϵ^a (kcal/mol)	r_0^b (Å)
OW–OW	0.093891	3.24
HW–HW	0.044252	2.83

^a ϵ is the depth of the energy minimum.

^b r_0 is the corresponding internuclear distance.

a translational vector $t^k = (t_1^k, t_2^k, t_3^k)$ and Eulerian angles $(\tau_1^k, \tau_2^k, \tau_3^k)$. Moreover, three internal variables in the k th water molecule are specified by two bond lengths (ρ_1^k for the O–H₁ distance and ρ_2^k for the O–H₂ distance) and a bond angle ρ_3^k . So, one water molecule has a total of nine d.f.

2.1.2. Total potential energy E of a water hexamer

The total potential energy E for a water hexamer is described as a sum of five terms as follows:

$$\begin{aligned}
 E = & \sum_{\text{pairs}} \frac{1}{4\pi\epsilon_0} \frac{q_i q_j}{r_{ij}} + \sum_{\text{pairs}} \left\{ \epsilon \left(\frac{r_0}{r_{ij}} \right)^{12} - 2.0\epsilon \left(\frac{r_0}{r_{ij}} \right)^6 \right\} \\
 & + \sum_{\text{H-bonds}} \left\{ \epsilon \left(\frac{r_0}{r_{HX}} \right)^{12} - 2.0\epsilon \left(\frac{r_0}{r_{HX}} \right)^{10} \right\} \\
 & + \frac{1}{2} \sum_{\text{waters } v=1}^3 \sum K_{vv} (\rho_v^k - \rho_{v,0})^2 \{1 + K_{vv}^{\text{cub}} (\rho_v^k - \rho_{v,0})\} \\
 & + \frac{1}{2} \sum_{\text{waters } \mu \neq v=1}^3 \sum K_{\mu v} (\rho_\mu^k - \rho_{\mu,0}) (\rho_v^k - \rho_{v,0}) \quad (1)
 \end{aligned}$$

The first three terms are intermolecular interaction terms. We briefly describe the terms [18] in Eq. (1). The first term is an electrostatic energy. The partial charges of a water oxygen (OW) and hydrogen (HW) are -0.330 and 0.165 , respectively, in electronic charge units. The second term is the nonbonded interaction energy of an atom pair i, j . The energy parameters are shown in Table 1. The third term is a hydrogen bond potential between donor (H) and acceptor (X) atoms. The energy parameters are shown in Table 2. The last two terms are intramolecular interaction terms. They represent a simple quadratic plus cubic potential function and cross terms for bond stretching and bond angle bending in the waters, respectively. $K_{\mu v}$ is a force constant for variables ρ_μ^k and ρ_v^k ; it is assumed to be the same for all water molecules. The $\rho_{v,0}$ ($v = 1, 2, \text{ or } 3$) is the equilibrium value for each variable ρ_v^k . K_{vv}^{cub} ($v = 1, 2, \text{ or } 3$) is a coefficient

Table 2

Hydrogen bond potential parameters $U_{HB} = \epsilon(r_0/r_{HX})^{12} - 2.0\epsilon(r_0/r_{HX})^{10}$		
Atom pairs (H, X)	ϵ (kcal/mol)	r_0 (Å)

HW–OW	0.843454	2.2063
	$4.29\epsilon^a = 3.6184$	$0.775r_0^b = 1.7099$

^a The depth of the energy minimum is 4.29ϵ .

^b The corresponding internuclear distance is $0.775r_0$.

Table 3
Intra-water potential parameters.

v	K_{v1}	K_{v2}	K_{v3}	K_{vv}^{cub}	$\rho_{v,0}$
1	1095 kcal/(mol Å ²)	−7.6 kcal/(mol Å ²)	5.0 kcal/(mol Å rad)	−8.0 (1/Å)	1 (Å)
2	−7.6	1095	5.0	−8.0 (1/Å)	1 (Å)
3	5.0	5.0	99.8 kcal/(mol rad ²)	1.1 (1/rad)	109.5°

expressing the magnitude of anharmonicity in the cubic potential term. These parameters [19] are listed in Table 3. The validity of using these intra-water potential parameters has already been demonstrated [19].

2.1.3. Hessian matrix for total potential energy E

The second derivative $\partial^2 E / \partial q_i \partial q_j$ for the total potential energy E can be summarized into a single formula as follows:

$$\frac{\partial^2 E}{\partial q_i \partial q_j} = (\phi_i, \psi_i) \left\{ s_{ij} \sum_{\xi \in M_i} \sum_{\eta \in M_j} (c_{\xi\eta} C_{ij}^* + d_{\xi\eta} D_{\xi\eta}) \right\} \times \begin{pmatrix} \phi_j \\ \psi_j \end{pmatrix} \quad (2)$$

Here q_i means the independent variables of each molecule within a hexamer. See [20] for the derivation of the Hessian matrix and a discussion of the terms in Eq. (2).

3. Results

We examine each of the water hexamer structures (cyclic, boat, book, prism and cage) in turn.

3.1. Cyclic hexamer

3.1.1. Energy minimization

The initial conformation of the cyclic hexamer is constructed from six water molecules H-bonding each other. The Hessian is expressed in terms of the nine d.f. mentioned earlier, making a total of 54 (9×6). This conformation is energy minimized using Newton's method based on a modified Cholesky factorization [21] of the Hessian. Energy minimization is stopped when the energy difference between the current step and the earlier step becomes less than 1×10^{-8} kcal/mol. At this point, the subset of the Hessian, whose elements are expressed in terms of t_v^k and τ_v^k had six positive eigenvalues. Likewise the subset expressed in terms of ρ_v^k had three positive eigenvalues.

3.1.2. Normal mode analysis

First, consider the rigid-body motions of the hexamer. The force constant matrix F of each rigid water molecule is the subset of the Hessian obtained at the energy minimum point, having six positive eigenvalues. The kinetic energy matrix H for a rigid water molecule expressed in terms of a translational vector and Eulerian angles is given in [22].

With the kinetic and force constant matrices (H and F), normal vibrational modes for each water molecule within the hexamer are obtained by solving the generalized eigenvalue equation

$$F \Delta u = (2\pi v_\alpha)^2 H \Delta u \quad (3)$$

where v_α is the frequency of the α th normal mode. The Δu is a six-dimensional column vector, whose elements are ($\Delta t_1, \Delta t_2, \Delta t_3, \Delta \tau_1, \Delta \tau_2, \Delta \tau_3$). This vector Δu expressing the changes of the translating vector and the Eulerian angles is converted into the changes Δr of atomic coordinates of the molecule by a series of mathematical manipulations, which are given in [22]. Thus the mean-square displacement matrix D of the i th atom caused by the rigid-body motions of a water molecule within the hexamer is obtained by

$$D = \begin{pmatrix} \langle \Delta x_i \Delta x_i \rangle & \langle \Delta x_i \Delta y_i \rangle & \langle \Delta x_i \Delta z_i \rangle \\ \langle \Delta y_i \Delta x_i \rangle & \langle \Delta y_i \Delta y_i \rangle & \langle \Delta y_i \Delta z_i \rangle \\ \langle \Delta z_i \Delta x_i \rangle & \langle \Delta z_i \Delta y_i \rangle & \langle \Delta z_i \Delta z_i \rangle \end{pmatrix} \quad (4)$$

The six vibrational frequencies of rigid-body motions for each water molecule within the hexamer are shown in Table 4. From the mean-square displacement matrix D , anisotropic thermal vibrations [23] for all hydrogens and oxygens in the cyclic hexamer are depicted in Fig. 2. In this figure as well as in subsequent figures, the displacements that occur when each of the six normal modes is thermally excited at 300 K are calculated. We see that free hydrogen atoms are fairly librating and all the ellipsoids of H-bonded hydrogen are small and thin, and their flat faces are perpendicular to the axes of H-bonding. This is reasonable because H-bonding restricts the motion of the hydrogens to the space between the pairs of oxygens. The ellipsoids of oxygen atoms contributing as acceptors are longer along the C₂-like axis of the water. As a criterion of H-bonding, we assume as before [1] that a hydrogen-acceptor distance must be less than 2.5 Å, and a donor-hydrogen-acceptor angle must be larger than 135°.

In analyzing the internal motions of each water molecule within the hexamer, the force constant matrix of the each molecule is the subset of the Hessian obtained at the energy minimum point, having three positive eigenvalues. The kinetic energy matrix for the water molecule expressed in terms of two bond lengths and a bond angle is given in [24]. With the kinetic and force constant matrices, normal modes for each water molecule are obtained by solving the generalized eigenvalue equation. The three internal frequencies for each water molecule are given in Table 5. We could also

Table 4

Vibrational frequencies for each of the six rigid water molecules within the hexamer (cm^{-1})

Type ^a							
Cyclic							
101		26	78	220	245	363	406
102		26	77	222	250	345	407
103		26	78	221	255	342	412
104		26	78	211	271	344	406
105		26	77	210	259	352	408
106		26	78	222	237	365	415
Boat							
201		21	71	215	285	310	381
202		22	84	199	241	370	415
203		22	82	208	241	354	415
204		21	72	230	272	315	388
205		22	85	187	276	347	411
206		22	82	210	257	339	403
Book							
301	d-D s-A	124	217	312	340	540	711
302		26	64	200	295	336	587
303		25	68	214	294	315	551
304	s-D d-A	172	249	260	311	370	739
305		27	84	232	296	324	461
306		26	61	209	298	305	569
Prism							
401	s-D d-A	189	217	232	285	500	805
402 ^b	<i>d-D s-A</i>	180	203	245	396	764	930
403	s-D d-A	179	209	239	281	431	847
404	<i>d-D s-A</i>	186	219	241	386	679	919
405	s-D d-A	197	201	241	299	431	817
406	<i>d-D s-A</i>	196	213	225	392	753	897
Cage							
501	s-D d-A	218	227	254	294	445	756
502	s-D d-A	212	227	253	297	442	704
503		31	59	223	283	396	541
504	<i>d-D s-A</i>	152	191	309	471	648	802
505	<i>d-D s-A</i>	192	232	280	385	691	777
506		37	57	211	278	403	628

^a s-D s-A unless otherwise noted.

^b Italics is used to distinguish the d-D s-A contacts.

calculate the thermal motions for each hydrogen and oxygen in the cyclic hexamer, though this is not shown in this article.

Note also the experimental values of the frequencies of the monomer in Table 5. There is excellent agreement between our calculations and experiment.

3.2. Boat hexamer

Using the same procedure as for the cyclic hexamer, predicted frequencies for the boat geometry were obtained (Tables 4 and 5). The thermal ellipsoids of rigid water molecules are depicted in Figs. 3 and 4. The boat shape is clear in Fig. 4. The motions of hydrogen and oxygen atoms are more or less similar to the those of the cyclic hexamer.

3.3. Book hexamer

Normal mode analysis gives the vibrational frequencies in Tables 4 and 5. The thermal ellipsoids of the book hexamer

Table 5

Internal frequencies for each of the six water molecules within the hexamer (cm^{-1})

Type ^a			
Cyclic			
101		1558	3654
102		1558	3654
103		1558	3654
104		1558	3654
105		1558	3654
106		1558	3654
Boat			
201		1561	3657
202		1558	3654
203		1557	3656
204		1561	3657
205		1558	3654
206		1557	3656
Book			
301	d-D s-A	1769	3628
302		1564	3598
303		1565	3610
304	s-D d-A	1543	3554
305		1568	3642
306		1572	3610
Prism			
401	s-D d-A	1555	3321
402	d-D s-A	1609	3471
403	s-D d-A	1561	3368
404	d-D s-A	1588	3430
405	s-D d-A	1555	3328
406	d-D s-A	1613	3474
Cage			
501	s-D d-A	1846	3411
502	s-D d-A	1892	3477
503		1573	3587
504	d-D s-A	1692	3578
505	d-D s-A	1601	3552
506		1945	3508
Monomer in gas phase ^b			
		1594	3654
Experimental data for monomer ^c			
		1594	3656

^a s-D s-A unless otherwise noted.

^b Calculated data to compare with the hexamer data. The data are from Table 2 of [19], where the data in the column “Harmonic” should be placed in the column marked “Anharmonic”.

^c See [25].

are shown in Fig. 5. We can see that the rigid-body motions of the water molecules labeled 301 and 304 are suppressed by three H-bonds; the former is acting as double donor, single acceptor (d-D s-A), and the latter is as s-D d-A. The ellipsoids are relatively small for these H-bonds; the lowest frequency mode of these two waters has much higher energy than do the modes for the s-D s-A waters, as the frequency values of Table 4 demonstrate. Free hydrogens of waters 302, 303 and 305 are somewhat librating, whereas for the 306 water molecule, the ellipsoids of free and H-bonded hydrogens are of similar size, even though the values of frequencies of 306 are close to those of 302, 303 and 305.

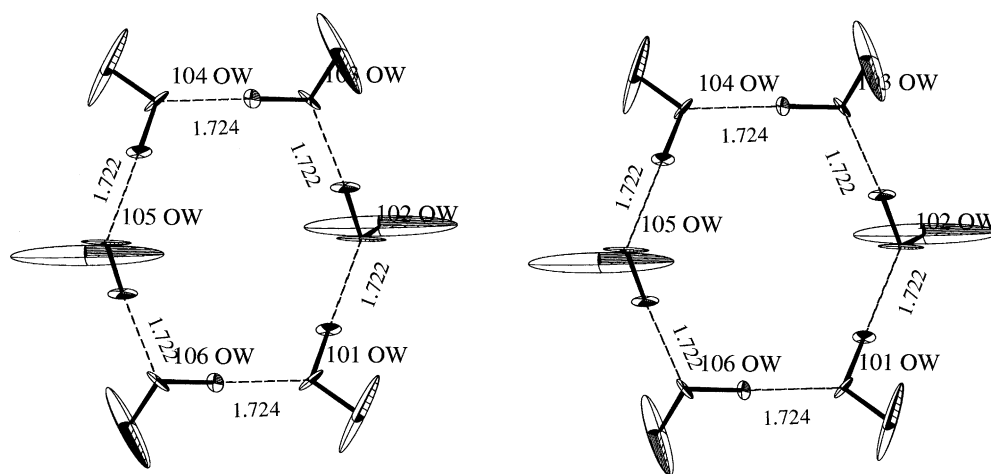


Fig. 2. Stereo view of rigid-body motions of each water molecule in the cyclic hexamer. The thermal ellipsoids of atoms (at 97% probability) are drawn in ORTEP. The dashed lines show six H-bonds. The numerical values are the distances (Å) between donor (HW) and acceptor (OW). All the water molecules are participating to H-bond as single-donor, single-acceptor (s-D s-A).

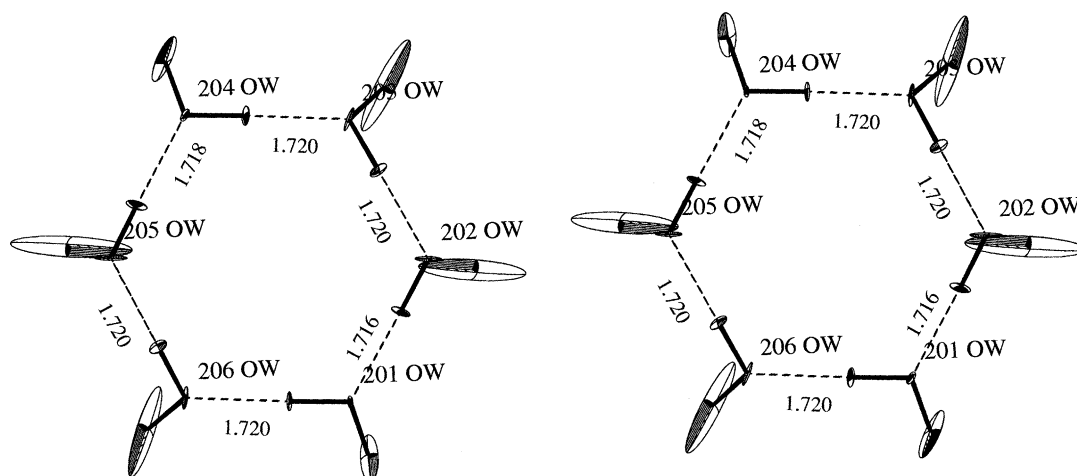


Fig. 3. Stereo view of rigid-body motions for the boat hexamer. Six H-bonds exist. All water molecules are of the type s-D s-A.

3.4. Prism hexamer

Normal mode analysis yields the frequencies listed in Tables 4 and 5. The thermal ellipsoids are also drawn in

Fig. 6. The ellipsoids of free hydrogens in the s-D d-A water molecules labeled 401, 403 and 405 are a little larger than those of hydrogens in the d-D s-A water molecules of 402, 404 and 406. The frequencies of the three higher modes of

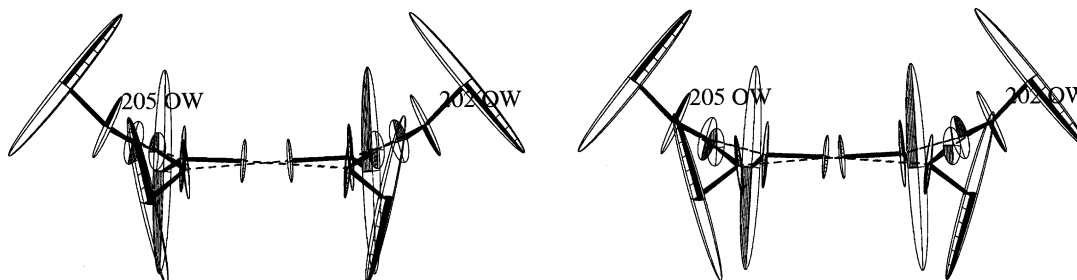


Fig. 4. Stereo view for the side view of rigid-body motions of the boat hexamer.

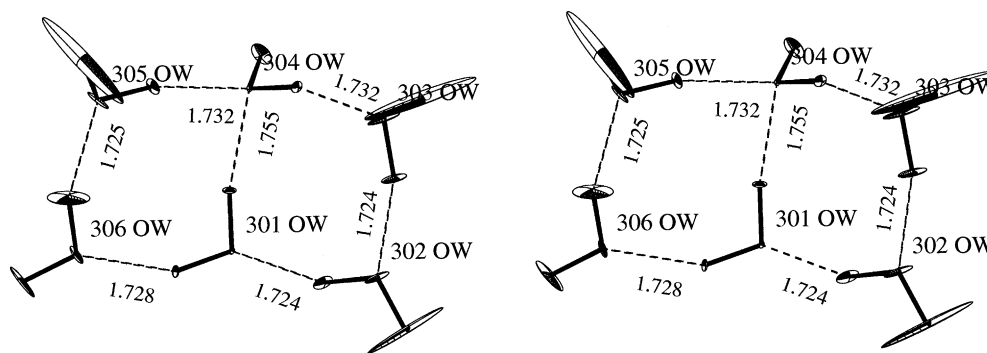


Fig. 5. Stereo view of rigid-body motions for the book hexamer. Seven H-bonds exist. The 301 water molecule is a double-donor, single-acceptor (d-D s-A), the 304 water is a single-donor, double-acceptor (s-D d-A), and the others are s-D s-A.

401, 403 and 405 are always lower than those of 402, 404 and 406.

3.5. Cage hexamer

The initial structure of a cage hexamer for our energy minimization is the one analyzed by Tsai and Jordan [4]. Normal mode analysis for the energy minimized conformation obtained produces the frequencies in Tables 4 and 5. The thermal ellipsoids are also depicted in Fig. 7. Free hydrogens in s-D s-A water molecules 503 and 506 are moderately librating. This is reflected by the lower vibrational frequencies of all six modes of these two waters compared to the respective frequencies of the other waters, as shown in Table 4.

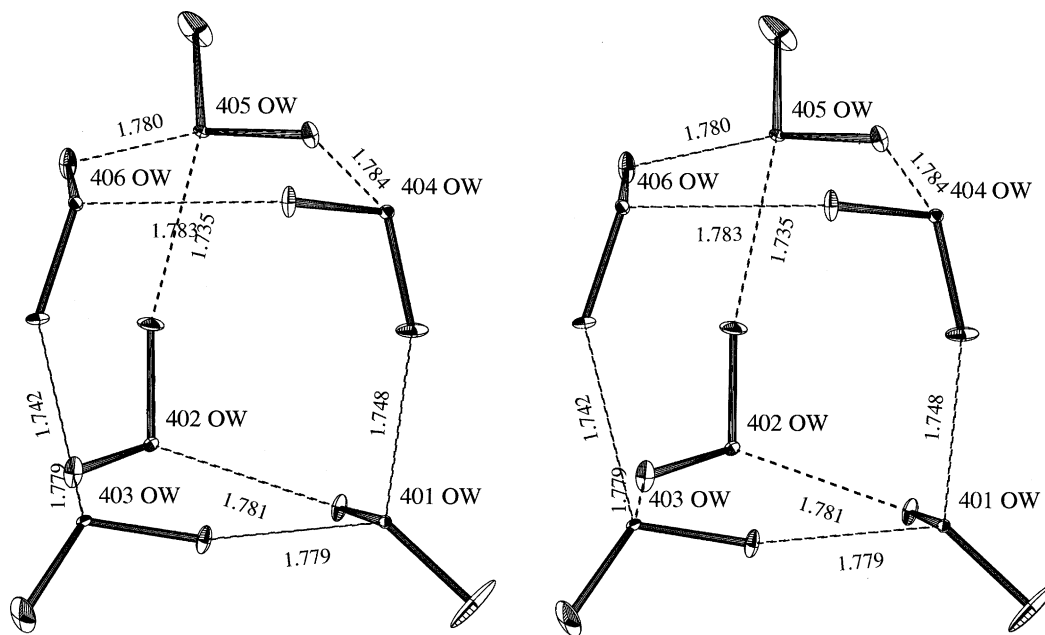


Fig. 6. Stereo view of rigid-body motions for the prism hexamer. Nine H-bonds exist. The 401, 403 and 405 water molecules are s-D d-A, and the 402, 404 and 406 waters are d-D and s-A. The $D(404\text{ OW})-H(404\text{ HW1})-A(406\text{ OW})$ angle is only 134° , but we accept it as an H-bond.

4. Discussion

4.1. Relationship between H-bond strength and H-bond lifetime

In the earlier article studying the interaction of a protein and water molecules surrounding the protein, we derived a relationship between H-bond strength and H-bond lifetime and found that a strong H-bond has a longer lifetime than a weak H-bond [1]. Here we investigate whether a relationship between H-bond strength and H-bond lifetime exists for the water hexamers.

First, we have to define an H-bond strength. This is given in [1], but we will briefly describe it below. There are two values characterizing an H-bond: the hydrogen-acceptor

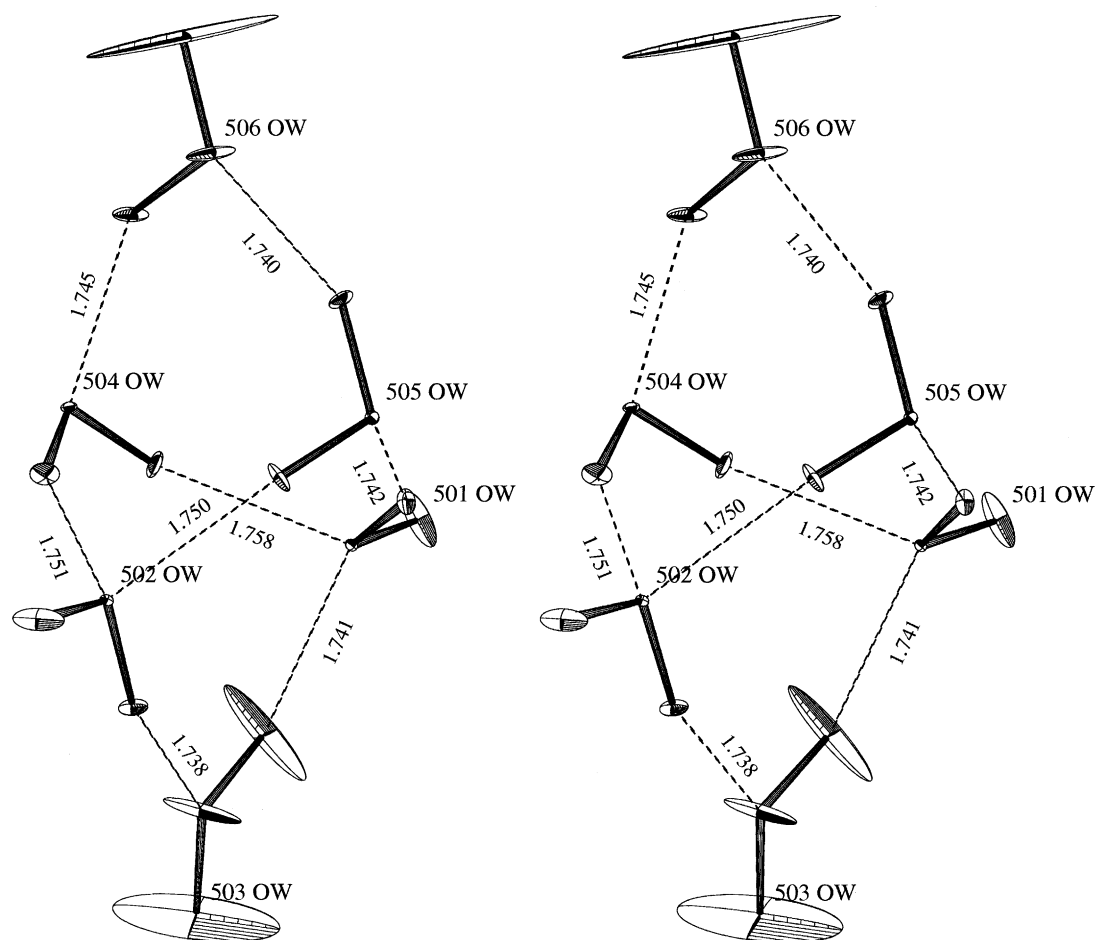


Fig. 7. Stereo view of rigid-body motions for the cage hexamer. Eight H-bonds exist. The 501 and 502 water molecules are s-D d-A, and the 504 and 505 waters are d-D s-A, and the others are s-D s-A.

distance (HAd) and the donor-hydrogen-acceptor angle (DHAA). An H-bond potential appearing in Eq. (1) has a minimum energy (of 4.29ϵ) at r_{\min} ($0.775r_0$), and then if HAd is equal to r_{\min} , the H-bonding is expected to be strong. On the other hand, the H-bond strength also depends on DHAA. If DHAA is equal to 180° , the H-bond strength is expected to be strong. Hence combining the both factors, we have assumed an H-bond strength is evaluated as follows (see Fig. 8). The vector from the minimum energy point to the acceptor has a height from the donor-hydrogen line, and the lower this height is, the stronger the H-bond strength; if the height is zero, the strength is maximized. Hence, H-bond strength was defined as $|HAd - r_{\min}| \times \sin(180^\circ - DHAA)$ and is greater when this quantity is smaller.

Second, we describe how we can estimate a duration time of H-bonding. Water's rigid-body motion sometimes breaks its H-bonds and rearranges the H-bonding patterns. In the independent MM, we obtain the six vibrational frequencies (v_i , $i = 1-6$) of the rigid-body molecules. The frequency fluctuation assigned as $\Delta v \approx (v_{\max} - v_{\min})/2$ corresponds to the energy fluctuation $\Delta E = h\Delta v$, where h is Planck's

constant. With the uncertainty relation, we can estimate the duration time $\Delta\tau$ of the rigid body in motion by its frequency fluctuation Δv as $\Delta\tau = 1/c\Delta v$, where c is the velocity of light (3.0×10^{10} cm/s).

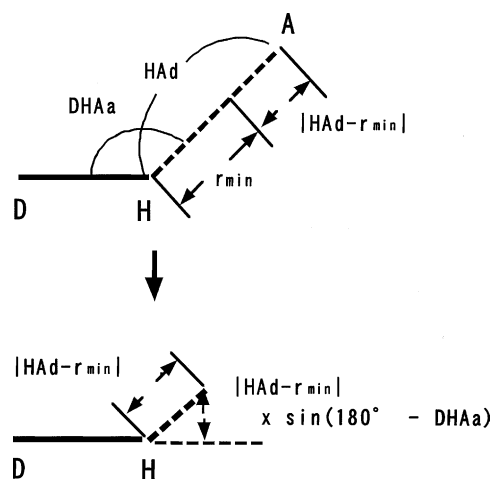


Fig. 8. Geometrical parameters affecting H-bond strength.

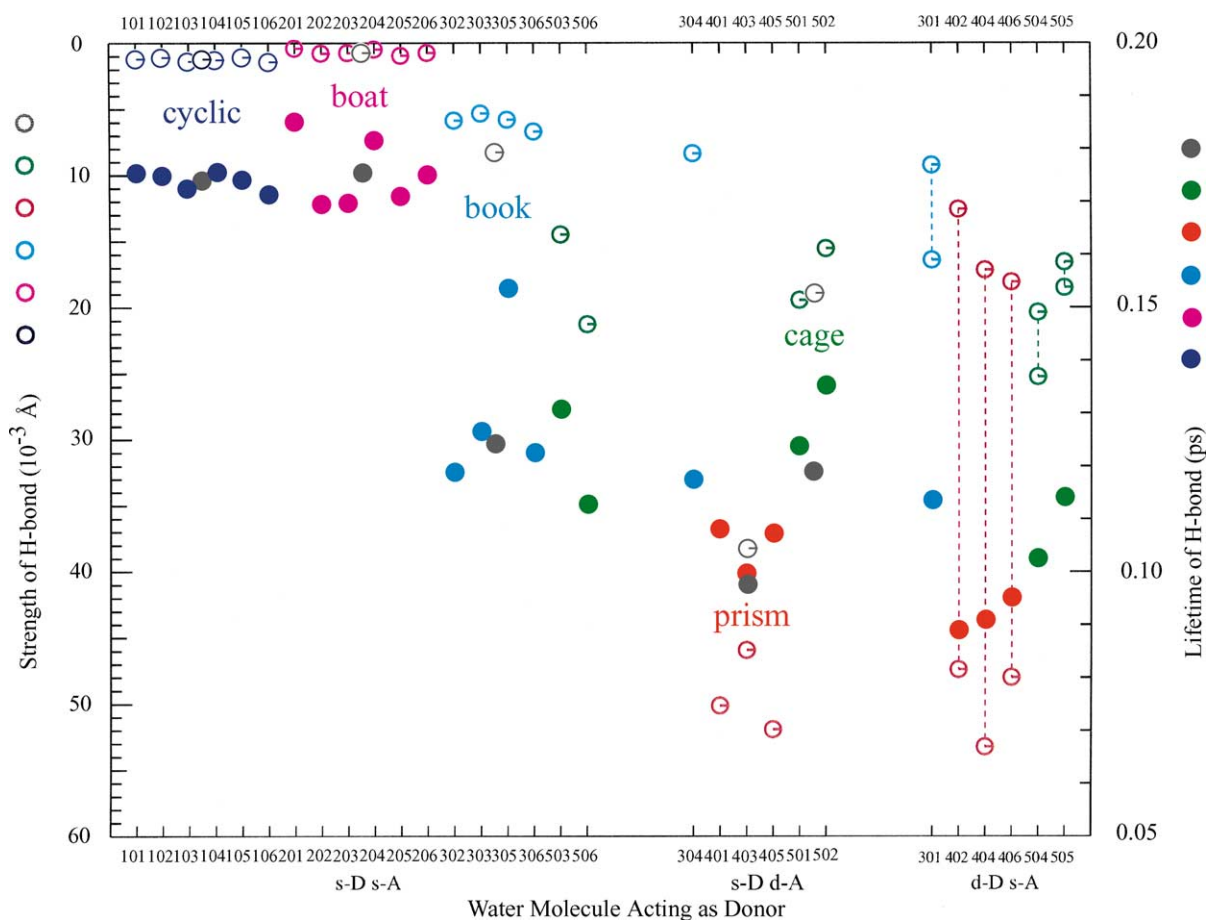


Fig. 9. Diagram of H-bond strength (open circles) and H-bond lifetime (solid circles) for water molecules acting as donor. The data points for each hexamer configuration are color coded: cyclic (blue), boat (magenta), book (aqua), prism (red) and cage (green). The left ordinate exhibits H-bond strength (in Å); the values become less positive as one goes up the axis; less positive means a stronger H-bond. Note that there are two strengths for d-D s-A zone. The gray open circles indicate the H-bond strengths averaged over each hexamer (zones of each color). The right ordinate describes H-bond lifetime (in ps). The gray solid circles indicate the H-bond lifetimes averaged over each hexamer.

In Fig. 9, diagrams of both H-bond strength and H-bond lifetime are described for the five hexamers. Note that each water molecule within the hexamer is acting as both donor and acceptor. In the hexamers analyzed here, each water molecule is contributing as s-D s-A, s-D d-A, or d-D s-A. When analyzing H-bond strength, we focus on donor H-bonds, not on acceptor H-bonds. Hence, in water molecules having a total of two H-bonds of s-D and s-A, only the strength of the donor H-bond is analyzed; in waters having three H-bonds of s-D and d-A, the strength of the donor H-bond is analyzed; and in waters having three H-bonds of d-D and s-A, the strengths of only the two-donor H-bonds are analyzed. On the other hand, regardless of whether the water molecule is H-bonded as s-D s-A, s-D d-A, or d-D s-A, the lifetime of H-bond is only one value because of its dependence on only rigid-body frequencies. In Fig. 9, we see that the H-bond strengths of all waters in the cyclic and boat hexamers are almost the same and are also stronger compared to those in the book, which in turn are stronger than those in the prism and cage. In the prism, although one H-bond in two-donor H-bonds

of d-D s-A waters is stronger than the other, the H-bond strength is not strong when averaged over the prism. On the other hand, H-bond lifetimes of all waters in the cyclic are almost the same, but those in the other four hexamers vary according to their locations within the hexamer. The H-bond lifetimes in four hexamers roughly cluster in three areas (longer, middle and shorter lifetime) in the order of boat (magenta), book (aqua), cage (green) and prism (red). In Table 6, we summarize both the H-bond strengths and lifetimes averaged over each hexamer.

From the data in Fig. 9, we discern a relationship: for a water molecule acting as donor H-bond, if its donor H-bond

Table 6
H-bond strength and H-bond lifetime averaged over each hexamer

	H-bond strength (Å)	H-bond lifetime (ps)
Cyclic	1.20×10^{-3}	0.174
Boat	0.69×10^{-3}	0.175
Book	8.24×10^{-3}	0.124
Prism	38.26×10^{-3}	0.097
Cage	18.92×10^{-3}	0.119

is stronger, the donor H-bond has a longer lifetime. On the other hand, if we focus on acceptor H-bond, what results do we see? Let us consider an H-bond as one example, say, the $D(301\text{ OW})\text{--}H(301\text{ HW1})\text{--}A(304\text{ OW})$ in Fig. 5. Up till now, we regarded this H-bond as a donor H-bond from the point of view of the 301 water. However, this H-bond is an acceptor H-bond from the point of view of the 304 water. The latter view corresponds to cataloging one of two H-bond strengths of 301 in the d-D s-A zone of Fig. 9 to 304 in the s-D d-A zone, so 301 loses one donor H-bond, while 304 gets another acceptor H-bond. This fact causes no essential changes to the substance of Fig. 9. The other five H-bonds (401 OW–404 HW2, 403 OW–406 HW2, 405 OW–402 HW2 in Fig. 6) and (501 OW–504 HW2, 502 OW–505 HW2 in Fig. 7) result in the same thing, and in addition, no changes happen in the s-D s-A zone of Fig. 9. Therefore, we can conclude that regardless of whether a water molecule is participating as a donor H-bond or an acceptor H-bond, the stronger its H-bond is, the longer the water conserves the H-bond. This conclusion is based on the five hexamers: whether this conclusion can be generalized to the other water clusters will be the subject of further study.

In the earlier article [1], we showed that for water molecules acting as the hydrogen acceptor from the protein, strong H-bonding has longer lifetimes than weak H-bonding. We could not demonstrate such a correlation for water molecules acting as H-bond donors to protein oxygens. This subject will be another problem for further investigation.

4.2. Free energy of the water hexamer

We are now in a position to estimate the Helmholtz free energy for each hexamer. We regard the water hexamer to be comprised of independent harmonic oscillators with the respective eigenfrequencies. Hence the partition function for the water hexamer, regarded as 6×6 harmonic oscillators for rigid-body motions and also as 3×6 oscillators for internal motions, is expressed as follows:

$$Z = e^{-\beta\Phi_0} \prod_{j=1}^{(6+3)\times 6} \frac{1}{2\sinh(\beta h\nu_j/2)} \quad (5)$$

where $\beta = 1/k_B T$ (k_B is the Boltzmann constant, T the absolute temperature), Φ_0 the potential energy of the water

hexamer at the energy minimum point, and ν_j is the j th eigenfrequency ($j = 1\text{--}9 \times 6$). With the partition function Z , the free energy is $F = -k_B T \log Z$, the internal energy is $U = -\partial \log Z / \partial \beta$, and the entropy is $S = -(\partial F / \partial T)_v$. Thus the internal energy is given as follows:

$$U = \Phi_0 + \sum_{j=1}^{(6+3)\times 6} \left\{ \frac{h\nu_j}{2} + \frac{h\nu_j}{e^{\beta h\nu_j} - 1} \right\} \\ = \Phi_0 + \epsilon_{\text{zero}}^{\text{rigid}} + \epsilon_{\text{osci}}^{\text{rigid}} + \epsilon_{\text{zero}}^{\text{int}} + \epsilon_{\text{osci}}^{\text{int}} \quad (6)$$

where the first term in the parentheses is the zero-point vibrational energy, and the second term is the average harmonic oscillator energy. The $\epsilon_{\text{zero}}^{\text{rigid}}$ and the $\epsilon_{\text{osci}}^{\text{rigid}}$ are the total zero-point vibrational energy and the total average harmonic oscillator energy for rigid-body motions, respectively, and the $\epsilon_{\text{zero}}^{\text{int}}$ and the $\epsilon_{\text{osci}}^{\text{int}}$ are those for internal motions. The entropy term TS is also given as follows:

$$TS = \frac{1}{\beta} \sum_{j=1}^{(6+3)\times 6} \left[\frac{\beta h\nu_j}{2} \coth \frac{\beta h\nu_j}{2} - \log \left\{ 2 \sinh \frac{\beta h\nu_j}{2} \right\} \right] \\ = (TS)^{\text{rigid}} + (TS)^{\text{int}} \quad (7)$$

where the $(TS)^{\text{rigid}}$ is the total vibrational entropy term for rigid-body motions, and the $(TS)^{\text{int}}$ is the one for internal motions. Thus the free energy F is expressed as $F = U - TS$, which is calculated as a sum of seven contributions. In Table 7, we show the free energy with the seven terms for each water hexamer at the temperature 300 K.

In Table 7, we see that the minimized energy Φ_0 corresponding to binding energy of the water hexamer increases in order: prism, cage, book, cyclic and boat. (In this paper, we use the terms “increases” and “decreases” in the algebraic sense, not necessarily in terms of the magnitudes.) Since the number of H-bonds in the hexamer is nine, eight, seven, six and six in this order, one would expect that the stabilization (binding energy) of the hexamer should decrease in this same order, and it does. As for the cyclic and the boat, the number of H-bond is the same, and the binding energy is the almost same. In addition, the values of the other terms in the free energy are also similar. So we regard the cyclic as the representative of these two. Contrary to order of Φ_0 , the increasing order of the free energy is: cyclic, book, cage, and prism, regardless of whether the free energy includes Φ_0 and just the rigid-body terms, or all terms.

Table 7
Free energy for the water hexamers at 300 K

	Φ_0	$+\epsilon_{\text{zero}}^{\text{rigid}}$	$+\epsilon_{\text{osci}}^{\text{rigid}}$	$-(TS)^{\text{rigid}}$	$+\epsilon_{\text{zero}}^{\text{int}}$	$+\epsilon_{\text{osci}}^{\text{int}}$	$-(TS)^{\text{int}}$	$F_0 = \Phi_0 + \text{rigid-body terms}$	$F = F_0 + \text{internal terms}$
Cyclic	−30.08	+11.43	+12.67	−28.61	+76.84	+0.02	−0.02	−34.59	42.25
Boat	−30.03	+11.24	+12.78	−29.38	+76.86	+0.02	−0.02	−35.40	41.46
Book	−32.60	+14.57	+11.18	−23.92	+76.36	+0.01	−0.02	−30.77	45.59
Prism	−34.89	+20.87	+8.55	−14.56	+73.94	+0.01	−0.02	−20.03	53.91
Cage	−34.73	+17.99	+9.56	−18.41	+76.69	+0.01	−0.01	−25.58	51.11

All terms are in unit of kcal/mol.

Let us survey the each term in the free energies of Table 7. The zero-point energy $\epsilon_{\text{zero}}^{\text{rigid}}$ decreases in the order: prism, cage, book, and cyclic, which is the direct result of rigid-body frequencies described in Table 4. Conversely, the average harmonic oscillator energy $\epsilon_{\text{osci}}^{\text{rigid}}$ decreases in the order: cyclic, book, cage, and prism, which is derived from the denominator of the second term in the parentheses of Eq. (6). The increasing order of the vibrational entropy term $-(TS)^{\text{rigid}}$ is cyclic, book, cage, and prism, which is a result of librational motions depicted in Figs. 2–7. The zero-point energy $\epsilon_{\text{zero}}^{\text{int}}$ for internal motions decreases in the order: cyclic, book, cage, and prism, which is inverse the order for rigid-body motions. The average harmonic oscillator energy $\epsilon_{\text{osci}}^{\text{int}}$ and the vibrational entropy term $(TS)^{\text{int}}$ for internal motions are tiny and contribute negligibly.

In Fig. 10, we summarize the temperature dependence of the free energy for the cyclic, cage, and prism hexamers.

For constructing this figure, we sum up the free energy to the rigid-body terms. The average harmonic oscillator energy $\epsilon_{\text{osci}}^{\text{rigid}}$ acts dramatically to make the structures less stable with increasing temperature. On the contrary, the entropy term $-(TS)^{\text{rigid}}$ acts dramatically to make the structures more stable. As already pointed out in Table 7, for data calculated at the 300 K, the prism (red) has the highest zero-point energy, and the higher the zero-point energy is, the more the average harmonic energy goes down because of the existence of the denominator ($e^{\beta h\nu} - 1$). The prism has the lowest harmonic oscillator energy and the greatest binding energy, but this more packed structure leads to less vibrational entropy and the entropy term of least magnitude. As a result, the prism hexamer is the least stable among three in the entire range of temperatures expressed in Fig. 10. As for the cyclic hexamer (blue), all the statements are opposite.

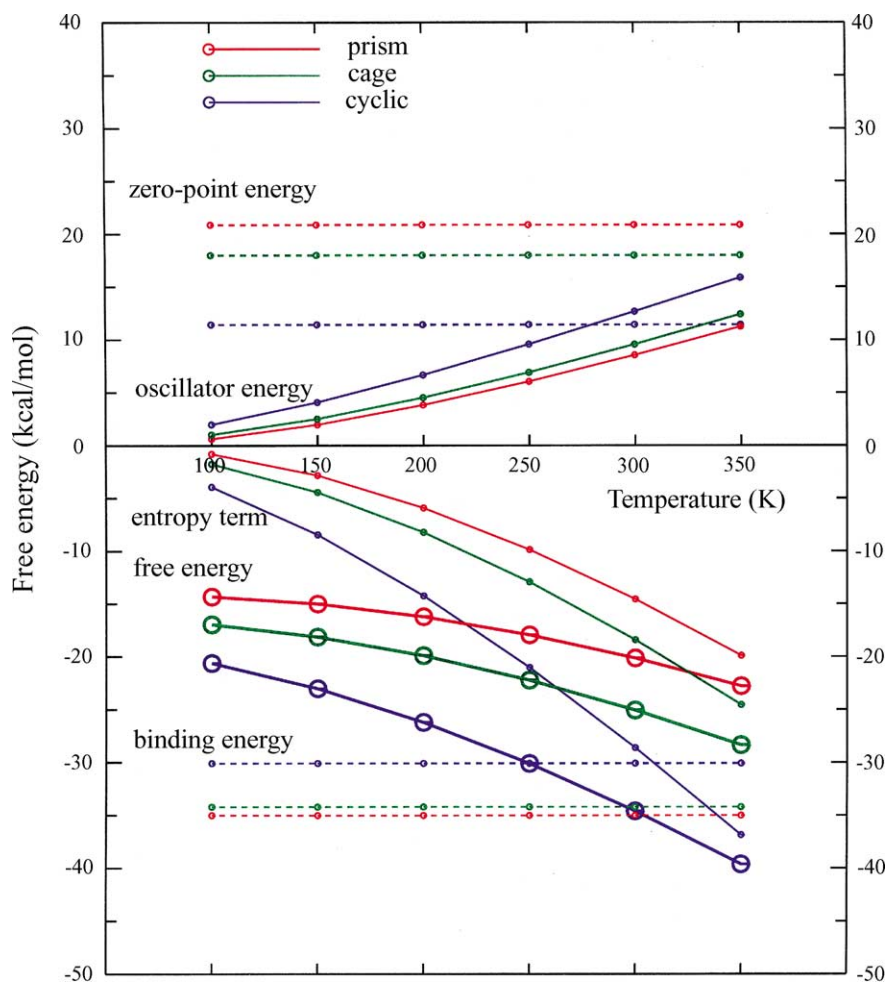


Fig. 10. Temperature dependence of the free energy for the water hexamers. The free energies consisting of up to rigid-body terms are plotted against the absolute temperature. The blue, green and red colors indicate the quantities relative to the cyclic, cage and prism hexamers, respectively. The lower dashed lines exhibit the binding energy Φ_0 , while the upper dashed lines exhibit the zero-point vibrational energy $\epsilon_{\text{zero}}^{\text{rigid}}$. The upper curves display the average harmonic oscillator energy $\epsilon_{\text{osci}}^{\text{rigid}}$, whereas the lower curves show the vibrational entropy term $-(TS)^{\text{rigid}}$. The thick curves with large open circles express the free energy. The data for the boat and book hexamers are not shown because the former is close to the data for the cyclic, and the latter is between the cyclic and the cage, as shown in Table 7.

5. Conclusions

The independent MM, devised to treat dynamics of a protein and water molecules interacting with the protein, has been utilized for water clusters. In this theoretical model, each molecule in the system has the six independent variables to ensure motions of molecule as a rigid body; each molecule can move into an energetic favorable site, being influenced by the potential fields of the other water molecules in the system. In addition, each molecule has three independent variables to permit its internal motions at each position of the molecule during the energy minimization process. Therefore each molecule is undergoing both the rigid-body motions and internal motions at the minimum point.

We have applied the model to the five water hexamers (cyclic, boat, book, prism and cage) in the gas phase. We have performed normal mode analyses on the five hexamers. With the frequencies of rigid-body motions, we have shown three main points. (1) As shown in Table 6, H-bond strength decreases in the order: boat, cyclic, book, cage and prism. (2) The H-bond lifetime decreases in this order, although the boat and the cyclic are almost the same. (3) As shown in Table 7 calculated at the 300 K, the free energy increases in this order as well. From Fig. 10, which exhibits the temperature dependence of the free energy, and Table 7, we see that the free energy for the boat is a bit lower than the cyclic and the ordering of the free energies is same throughout the temperature range of Fig. 10.

From the three points discussed above, we conclude that the boat hexamer is the most stable among the five hexamers in the gas phase. The boat cluster can preserve the H-bonds a longer time. Free energy, H-bond strength, and H-bond lifetime are closely related to each other because they all reflect stabilization of the interactions. As data of Tables 6 and 7 show, the stabilizing components of the free energy of the cyclic are a bit lower compared to the boat. As for the prism, its components are much smaller compared to the cyclic, while the stabilities of the book and cage are between the cyclic and the prism, but the book is slightly nearer to the cyclic, and the cage is somewhat nearer to the prism. The roughly planar configuration is the cyclic; the somewhat planar structure is the boat and is the most stable. The least planar structure is the prism, and it is the least stable. Our findings are for a water hexamer in the gas phase; in bulk water the situation may differ (e.g. see Fig. 7 in ref. [22]). This will be an important subject for future investigation.

Going back to the experiments of Liu et al. [14] these authors alleged that both the cage and boat structures are candidates to explain the experimental values, and the authors picked the cage. Our work suggests that the water hexamer most likely to be producing the experimental observations is the boat, since the boat would the most stable hexamer as described by our analyses.

So far, the independent MM has offered plenty of useful results from a molecular point of view. The leading quantities used with the analyses are the frequencies of rigid-body

motions and not those for internal motions. Hence the independent molecule model presenting the rigid-body frequencies is helpful for delineating dynamics of a multi-molecule system, for estimating a relationship between energy and lifetime, and for understanding free energy contributions.

Acknowledgements

The author thanks Dr. K.D. Jordan for providing the atomic coordinates of cage hexamer.

References

- [1] S. Yoshioki, Dynamics of a protein and water molecules surrounding the protein: Hydrogen-bonding between vibrating water molecules and a fluctuating protein, *J. Comput. Chem.* 23 (2002) 402–413.
- [2] K.S. Kim, M. Dupuis, G.C. Lie, E. Clementi, Revisiting small clusters of water molecules, *Chem. Phys. Lett.* 131 (1986) 451–456.
- [3] N. Pugliano, R.J. Saykally, Measurement of quantum tunneling between chiral isomers of the cyclic water trimer, *Science* 257 (1992) 1937–1940.
- [4] C.J. Tsai, K.D. Jordan, Theoretical study of the $(\text{H}_2\text{O})_6$ cluster, *Chem. Phys. Lett.* 213 (1993) 181–188.
- [5] S.S. Xantheas, T.H. Dunning Jr., The structure of the water trimer from ab initio calculations, *J. Chem. Phys.* 98 (1993) 8037–8040.
- [6] S.S. Xantheas, T.H. Dunning Jr., Ab initio studies of cyclic water clusters $(\text{H}_2\text{O})_n$, $n = 1$ –6. Optimal structures and vibrational spectra, *J. Chem. Phys.* 99 (1993) 8774–8792.
- [7] K. Kim, K.D. Jordan, T.S. Zwier, Low-energy structures and vibrational frequencies of the water hexamer: Comparison with benzene- $(\text{H}_2\text{O})_6$, *J. Am. Chem. Soc.* 116 (1994) 11568–11569.
- [8] R.N. Pribble, T.S. Zwier, Size-specific infrared spectra of benzene- $(\text{H}_2\text{O})_n$ clusters ($n = 1$ –7): Evidence for noncyclic $(\text{H}_2\text{O})_n$ structures, *Science* 265 (1994) 75–79.
- [9] S.S. Xantheas, Ab initio studies of cyclic water clusters $(\text{H}_2\text{O})_n$, $n = 1$ –6. III. Comparison of density functional with MP2 results, *J. Chem. Phys.* 102 (1995) 4505–4517.
- [10] D.A. Estrin, L. Paglieri, G. Corongiu, E. Clementi, Small clusters of water molecules using density functional theory, *J. Phys. Chem.* 100 (1996) 8701–8711.
- [11] J.D. Cruzan, L.B. Braly, K. Liu, M.G. Brown, J.G. Loeser, R.J. Saykally, Quantifying hydrogen bond cooperativity in water: VRT spectroscopy of the water tetramer, *Science* 271 (1996) 59–61.
- [12] K. Liu, M.G. Brown, J.D. Cruzan, R.J. Saykally, Vibration–rotation tunneling spectra of the water pentamer: Structure and dynamics, *Science* 271 (1996) 62–64.
- [13] K. Liu, D.C. Cruzan, R.J. Saykally, Water clusters, *Science* 271 (1996) 929–933.
- [14] K. Liu, M.G. Brown, C. Carter, R.J. Saykally, J.K. Gregory, D.C. Clary, Characterization of a cage form of the water hexamer, *Nature* 381 (1996) 501–503.
- [15] J.K. Gregory, D.C. Clary, K. Liu, M.G. Brown, R.J. Saykally, The water dipole moment in water clusters, *Science* 275 (1997) 814–817.
- [16] M.G. Gruenloh, J.R. Carney, C.A. Arrington, T.S. Zwier, S.Y. Fredericks, K.D. Jordan, Infrared spectrum of a molecular ice cube: the S₄ and D_{2d} water octamers in benzene- $(\text{water})_8$, *Science* 276 (1997) 1678–1681.
- [17] M. Masella, J.P. Flament, A pairwise and two many-body models for water: Influence of nonpairwise effects upon the stability and geometry of $(\text{H}_2\text{O})_n$ cyclic ($n = 3$ –6) and cagelike ($n = 6$ –20) clusters, *J. Chem. Phys.* 107 (1997) 9105–9116.

- [18] S. Yoshioki, Internal dynamics of a globular protein under external force field, *J. Comput. Chem.* 15 (1994) 684–703.
- [19] S. Yoshioki, Internal motions of a protein and surrounding water molecules, *J. Phys. Soc. Jpn.* 66 (1997) 2936–2947.
- [20] S. Yoshioki, Formulation of the hessian matrix for the conformational energy of protein–water systems, *J. Phys. Soc. Jpn.* 66 (1997) 2927–2935.
- [21] P.E. Gill, W. Murray, M.H. Wright, *Practical Optimization*, Academic Press, London, 1981, p. 105.
- [22] S. Yoshioki, Motions of water molecules surrounding a rigid protein model, *J. Phys. Soc. Jpn.* 67 (1998) 1477–1485.
- [23] C.K. Johnson, ORTEP: a Fortran Thermal Ellipsoid Plot Program, ORNL-3794, Oak Ridge National Laboratory, Oak Ridge, USA, 1965.
- [24] E.B. Wilson, Some mathematical methods for the study of molecular vibrations, *J. Chem. Phys.* 9 (1941) 76–84.
- [25] D.M. Ferguson, Parameterization and evaluation of a flexible water model, *J. Comput. Chem.* 16 (1995) 501–511.